

Soft-x-ray investigation of Mg and Al oxides: Evidence for atomic and bandlike features

W. L. O'Brien,* J. Jia, Q-Y. Dong, and T. A. Callcott
University of Tennessee, Knoxville, Tennessee 37996

D. R. Mueller and D. L. Ederer†
National Institute of Standards and Technology, Gaithersburg, Maryland 20899

C-C. Kao
Brookhaven National Laboratory, Upton, New York 11973
(Received 16 November 1992; revised manuscript received 1 February 1993)

Soft-x-ray emission (SXE) and soft-x-ray absorption (SXA) are used to investigate the electronic structure of α -Al₂O₃, anodized Al₂O₃, MgO, and MgAl₂O₄. It is found that both SXE and SXA are sensitive to the crystal phase, suggesting their use as a structural probe. Comparison of the Al *L*_{2,3} SXE of α -Al₂O₃ and the Mg *L*_{2,3} SXE of MgO with local-density-approximation (LDA) density-of-states calculations shows that the agreement is good, and suggests that the final-state rule is valid for the SXE of these oxides. On the other hand, comparisons show that results of the SXA and LDA calculations are not in good agreement. A model based on atomiclike excitations explains a portion of the MgO SXA spectrum well. Evidence which suggests that the remaining features are due to band structure is given.

INTRODUCTION

Soft-x-ray emission (SXE) and soft-x-ray absorption (SXA) are complementary techniques used to investigate electronic properties of materials. These two spectroscopies are especially useful in the study of insulators, since both can be accomplished by monitoring emitted photons which are not affected by sample charging. In SXE spectroscopy a core hole is created by either an incident electron or photon. This core hole state can relax by a radiative transition involving a valence electron. The energy distribution of these emitted photons, the SXE spectrum, is a measure of the occupied electronic density of states (DOS) on an energy scale relative to the core hole binding energy. In SXA the absorption is measured for photon energies above a core hole binding energy. This can be accomplished by monitoring the electron yield or reflectivity as the incident photon energy is changed. Changes in the absorption for energies above a core hole binding energy are dominated by matrix elements coupling core electrons to unoccupied states. SXA is thus a measure of the unoccupied DOS on an energy scale relative to the core electron binding energy.

Both SXE and SXA are sensitive to the local and partial DOS. The local nature is due to the involvement of a core state in the radiative transitions. The partial nature is a result of the dipole selection rule. For example the SXE of Al₂O₃ at photon energies near the Al *L*_{2,3} binding energy would give a measure of the Al *s* + *d* occupied DOS. Similarly, the SXA near the O *K* binding energy would give a measure of the O *p* unoccupied DOS. In principle, a complete measurement of both the occupied and unoccupied electronic DOS of each symmetry, centered on different atomic sites, can be made. This information allows a more thorough comparison with theory than techniques which measure the total DOS, such as

photoemission, or the joint DOS, such as optical reflectivity. Information of this type is also useful in determining bonding characteristics.

The effects of the core hole, the initial state in SXE, and the final state in SXA, need to be considered when discussing SXE and SXA spectra. Are the DOS's measured by these techniques influenced by the presence of the core hole? This question has been answered, for the case of simple metals,^{1,2} by both theoretical argument^{1,2} and by comparison of experiment with theoretical calculation.¹ It is found that SXE measures the DOS with no influence from the core hole, while SXA measurements are influenced by the presence of the core hole. These properties are described by the "final-state rule," which states that the DOS measured is that of the final state of the transition. Calculations of the ground-state DOS are useful for comparison to SXE, while calculations of the DOS in the vicinity of a core hole are needed for comparison to SXA. The SXE experiments^{1,2} discussed above were performed with electron-beam excitation. More recent work on the SXE of semiconductors³ and insulators⁴ using synchrotron radiation shows a photon energy dependence on the SXE spectrum for photon excitation energies near threshold. At photon excitation energies high above threshold the SXE spectrum is similar to the electron excited spectrum.³ In the work presented below electron-beam excitation is used.

In this paper we present and discuss SXE and SXA spectra of α -Al₂O₃, anodized Al₂O₃, MgO, and MgAl₂O₄. For α -Al₂O₃ each Al atom is in a near octahedral⁵ environment while the Al atoms in anodized Al₂O₃ are in tetrahedral sites. MgO crystallizes in the NaCl structure so that each Mg atom is in an octahedral site. The MgAl₂O₄ used was a true spinel with each Al atom in an octahedral site and each Mg atom in a tetrahedral site.⁵ Comparisons of the Al *L*_{2,3} SXE of α -Al₂O₃, anodized

Al_2O_3 and MgAl_2O_4 , the Al $L_{2,3}$ SXA of $\alpha\text{-Al}_2\text{O}_3$ and MgAl_2O_4 , and the Mg $L_{2,3}$ SXA of MgO and MgAl_2O_4 are made. These comparisons show the sensitivity of both SXA and SXE to the crystal phase and demonstrate that each technique can be used as a structural probe. Comparison of the MgO and $\alpha\text{-Al}_2\text{O}_3$ SXE and SXA spectra to local-density-approximation (LDA) calculations by Xu and Ching⁵ are made. Good agreement is found for the SXE results, suggesting that the final-state rule is valid for the SXE of these oxides. On the other hand, the agreement between SXA and the calculations of Xu and Ching are not good. The MgO SXA spectrum can be partially explained by a model considering atomic-like excitations, crystal-field splitting, and phonon broadening. Evidence that suggests that the remaining features are due to band structure is given.

EXPERIMENT

The experiments were performed on the University of Tennessee and National Institute of Standards and Technology soft-x-ray-emission spectrometer⁶ located at the National Synchrotron Light Source, Brookhaven National Lab. The spectrometer consists of a set of three interchangeable toroidal gratings and a position sensitive detector which scans the Rowland circle defined by the grating and an entrance slit. The resolution of the device was <0.2 eV for the experiments reported here. The $\alpha\text{-Al}_2\text{O}_3$, MgO, and MgAl_2O_4 samples were all high-purity cut and polished single crystals. The anodized Al_2O_3 was a polycrystalline film grown by anodizing aluminum metal. These samples were all mounted on a stainless-steel manipulator capable of positioning each sample in front of the spectrometer entrance slit. The sample in front of the slit could be irradiated by electrons or by white light from the synchrotron. The pressure in the chamber during the experiments was 2×10^{-10} Torr.

The SXE was accomplished by electron-beam excitation. Typical electron energies and currents used were 1 keV and 10 μA . The SXA was measured in the following manner. White light from the synchrotron was reflected specularly off the sample and into the spectrometer. The angle of incidence for this reflection was 15° off normal. The reflection spectrum was converted into an absorption spectrum using the following relationship:

$$R = \frac{(n-1)^2 + k^2}{(n+1)^2 - k^2},$$

where R is the measured reflectivity and n and k are the real and imaginary parts of the complex index of refraction. Under the conditions when $n \approx 1$ and $k \ll 1$, $R \propto k^2$, or within the same approximation, $R \propto \epsilon_2^2$, where ϵ_2 is the imaginary part of the dielectric function, which is proportional to the optical-absorption coefficient over a limited range of photon energies. We⁷ have previously made comparisons of the absorption spectra of $\alpha\text{-Al}_2\text{O}_3$ and MgO obtained in this manner with absorption spectra obtained using more conventional techniques and have found excellent agreement. The advantage of the reflection method is that the same spectrometer can be

used for absorption and emission measurements and that sample charging is not a problem.

RESULTS

The Al $L_{2,3}$ SXE spectra for $\alpha\text{-Al}_2\text{O}_3$, anodized Al_2O_3 , and MgAl_2O_4 are shown in Fig. 1. These spectra have each been divided by E^3 , where E is the photon energy so that comparison can be made to DOS calculations. The factor of E^3 comes from the dipole approximation and the photon density-of-states contribution to the transition rate. The emission spectrum for each compound consists of a double-peaked structure but with a different width and intensity ratio for the two peaks. The width of the valence band is greatest for $\alpha\text{-Al}_2\text{O}_3$ and smallest for MgAl_2O_4 . For each spectrum the energy position of the valence-band maximum is the same and the difference in valence-band widths is due to changes near the bottom of the valence band. The relative intensity of the lower energy peak is greatest for MgAl_2O_4 and least for $\alpha\text{-Al}_2\text{O}_3$.

The Al $L_{2,3}$ SXA spectra for $\alpha\text{-Al}_2\text{O}_3$ and MgAl_2O_4 are shown in Fig. 2. We were unable to obtain a SXA spectrum of anodized Al_2O_3 by reflectivity due to the roughness of the surface. The feature near 76 eV in the MgAl_2O_4 spectra is due to Mg $L_{2,3}$ absorption (based on comparison with the SXA of MgO). The two Al $L_{2,3}$ SXA spectra are similar but differ in detail. Each has a strong feature at threshold which has been identified as the core exciton.⁷ The exciton is resolved as a doublet in the $\alpha\text{-Al}_2\text{O}_3$ SXA spectrum. Each spectrum also contains a number of high-energy excitations between 90 and 105 eV. In Fig. 3 the Mg $L_{2,3}$ SXA of MgO and MgAl_2O_4 are shown. The features near 78 and 80 eV in the MgAl_2O_4 spectra are due to Al $L_{2,3}$ absorption (based on comparison with the SXA of $\alpha\text{-Al}_2\text{O}_3$). These two Mg $L_{2,3}$ spectra are also similar but differ in detail. The peak at threshold has been identified as the core exciton.⁷ It is apparent from Figs. 1–3 that both SXE and SXA can be used as a structural probe for these types of oxides.

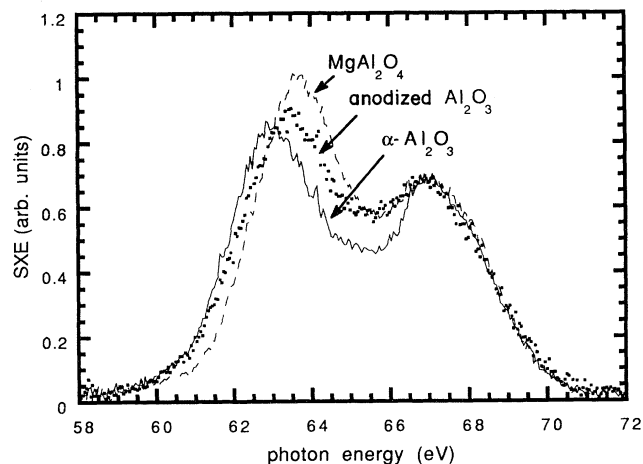


FIG. 1. Al $L_{2,3}$ SXE of $\alpha\text{-Al}_2\text{O}_3$, solid line; anodized Al_2O_3 , dots; and MgAl_2O_4 , dashed line. The spectra have been divided by E^3 and normalized at 67 eV.

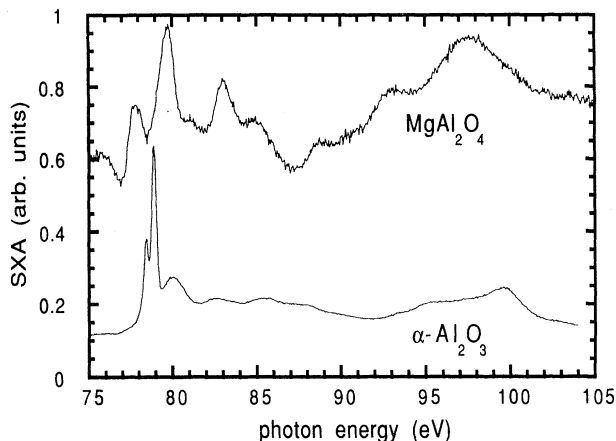


FIG. 2. Al $L_{2,3}$ SXA of MgAl_2O_4 (top) and $\alpha\text{-Al}_2\text{O}_3$ (bottom). The feature at 76 eV in the MgAl_2O_4 spectra is due to Mg $L_{2,3}$ absorption. The spectra have been displaced vertically for comparison.

In order to better understand the SXE and SXA results, comparison is made with DOS calculations by Xu and Ching⁵ using the local-density approximation (LDA). These are ground-state calculations (no core hole) and do not contain matrix element effects which might be important in SXE. Figure 4 compared the calculated DOS curves of MgO and $\alpha\text{-Al}_2\text{O}_3$ with the SXE results. The SXE spectra are energy shifted to achieve best alignment. The low-energy peak in the MgO SXE spectra is due to a core-core transition, $L_1\text{-}L_{2,3}$, and will not be contained in the LDA calculation. The calculated DOS curves shown in Fig. 4 were determined from the results of Xu and Ching⁵ in the following manner. The s and d symmetry-projected DOS's were added together and broadened by convolution with a Gaussian function, and the spin-orbit splitting of the $L_{2,3}$ state was also accounted for. The Gaussian broadening approximates the strong phonon coupling in these oxides.⁸ Gaussians of full width at half

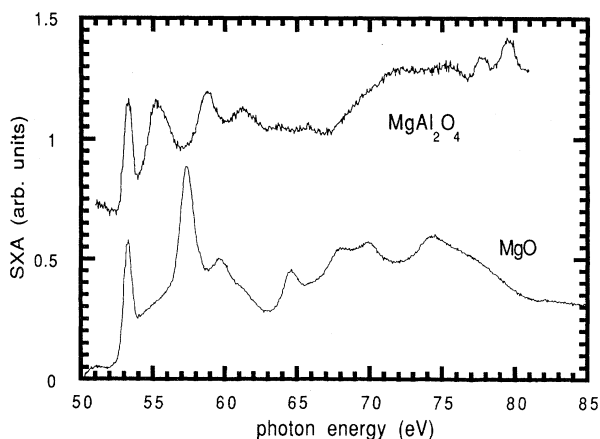


FIG. 3. Mg $L_{2,3}$ SXA of MgAl_2O_4 (top) and MgO (bottom). The features near 78 and 80 eV in the MgAl_2O_4 spectrum are due to Al $L_{2,3}$ absorption. The spectra have been displaced vertically for comparison.

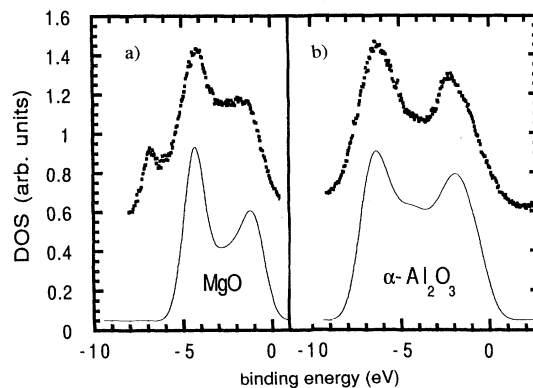


FIG. 4. (a) Mg $L_{2,3}$ SXE/ E^3 of MgO (top) compared to LDA calculations of Xu and Ching (Ref. 5) (bottom). (b) Al $L_{2,3}$ SXE/ E^3 of $\alpha\text{-Al}_2\text{O}_3$ (top) compared to LDA calculations of Xu and Ching (Ref. 5) (bottom). The energy positions of the SXE spectra in both (a) and (b) have been shifted to achieve the best comparison with the calculated density of states. The lowest-energy feature in the MgO SXE spectrum is a core-core radiative transition and should not appear in the DOS calculation.

maximum of 1.5 and 1.0 eV were used for $\alpha\text{-Al}_2\text{O}_3$ and MgO, respectively. Atomic values,⁹ 0.28 and 0.43 eV for MgO and $\alpha\text{-Al}_2\text{O}_3$, respectively, were used for the spin-orbit splitting. The statistical intensity ratio was used for the relative intensity of the L_2 and L_3 core states.

The MgO and $\alpha\text{-Al}_2\text{O}_3$ SXE spectra, both experimental and calculated, consist primarily of two peaks (Fig. 4). The calculations of Xu and Ching⁵ predict the relative intensities of the two peaks in the SXE of MgO and $\alpha\text{-Al}_2\text{O}_3$ well. The separation in energy of the two peaks is ≈ 0.5 eV greater in the calculations of Xu and Ching than in our SXE measurements for both MgO and $\alpha\text{-Al}_2\text{O}_3$. There is evidence of a third peak between the two primary peaks in the $\alpha\text{-Al}_2\text{O}_3$ SXE spectrum. This feature is present in the calculation. Xu and Ching⁵ also predict that the valence-band width of MgAl_2O_4 is intermediate between the valence-band width of MgO and $\alpha\text{-Al}_2\text{O}_3$; this is supported by our measurements. We feel these calculations describe well the SXE of these oxides. These comparisons give support for the final-state rule in the SXE from these oxides and also suggest that the dipole matrix element does not change much in magnitude in the energy range of SXE for aluminum and magnesium.

In Fig. 5 the SXA spectra of MgO and $\alpha\text{-Al}_2\text{O}_3$ are compared to the LDA calculations of Xu and Ching⁵ of the conduction-band states. The s and d symmetry-projected conduction-band densities of states have been treated in the same manner as the valence-band states for comparison to measurement. The SXA spectra have been energy shifted to achieve the best lineup of features above threshold. These calculations will not include the core exciton since they are ground-state calculations. For MgO the experimental feature near 4 eV has been aligned with the higher-energy feature in the LDA calculation (Fig. 5). There is no feature in the experimental spectrum to correspond to the peak nearest threshold in

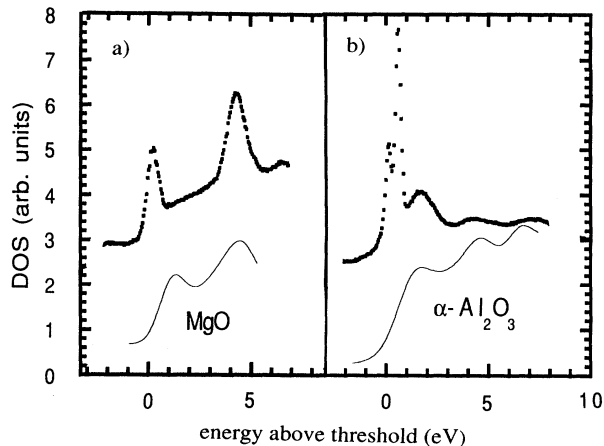


FIG. 5. (a) Mg $L_{2,3}$ SXA of MgO (top) compared to LDA calculations of Xu and Ching (Ref. 5) (bottom) (b) Al $L_{2,3}$ SXA of α -Al $_2$ O $_3$ (top) compared to LDA calculations of Xu and Ching (Ref. 5) (bottom). The energy positions of the SXA spectra in both (a) and (b) have been shifted to achieve the best comparison with the density-of-states calculations.

the calculated spectra. For α -Al $_2$ O $_3$ the calculated and experimental (not counting the exciton doublet) spectra each contain three peaks near threshold. In Fig. 5 the α -Al $_2$ O $_3$ SXA spectrum is energy shifted to align the first peak above threshold with the calculated spectrum. The second peak above threshold in the SXA spectrum is 0.5 eV lower in energy than in the calculated spectrum, while the third peak is 0.5 eV higher in energy. The separation of these two peaks is thus 1.0 eV greater in our SXA measurement than in the calculation. Also, the intensity ratio of the three peaks is much different in the calculated and experimental spectra. Since the LDA calculations⁵ on MgO and α -Al $_2$ O $_3$ are performed up to energies \approx 10 eV above threshold, comparison with the features farther above threshold is not possible. We feel the comparison between theory and experiment for the SXA is worse than for SXE.

To further understand the SXA we have made comparisons with a model based on atomiclike excitations. MgO is highly ionic and the Mg atom is well described as being doubly ionized. The bottom of Fig. 6 shows the Mg $L_{2,3}$ absorption spectrum for the free Mg $^{2+}$ ion. The energy positions are taken from measurements compiled by Moore⁹ and the intensities are from calculations by Gruzdev and Loginov.¹⁰ The peak at 53.5 eV is due to transitions from the core state into the 3s level. This appears as a single peak rather than a doublet since the LS coupling limit is valid. The transitions at higher energies in the free Mg $^{2+}$ ion are due to transitions into the nd states, where $n=3, 4, 5$. The ionization threshold is near 80 eV. Two solid-state effects on transitions of this type are phonon broadening and splitting of the d levels by the crystal field. We have approximated the phonon broadening by Gaussian convolution and assumed a crystal-field splitting of 4 eV. Comparison of this result (middle curve in Fig. 6), to the Mg $L_{2,3}$ SXA of MgO (top curve in Fig. 6) suggests that the feature at threshold and

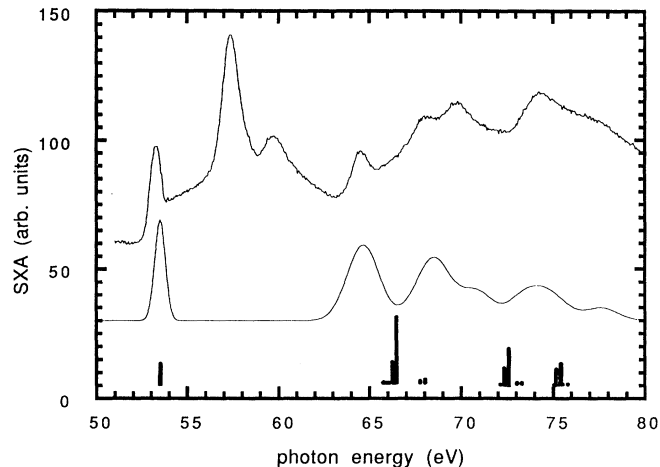


FIG. 6. SXA of the free Mg $^{2+}$ ion (bottom). Effects of phonon broadening and crystal-field splitting on free-ion SXA (middle). Mg $L_{2,3}$ SXA of MgO (top).

the features located more than 10 eV above threshold are due to atomiclike excitations. We feel an even better comparison would be obtained if the electrostatic contributions to the Hamiltonian were allowed to mix the crystal-field-split levels.^{11,12} It is important to note that the energy scales in Fig. 6 are not shifted to achieve best alignment. Both the exciton and the higher-energy absorption features are well explained in terms of atomiclike transitions. This is reasonable since both the exciton state and the d states are highly localized in the solid.

Since MgAl $_2$ O $_4$ is also highly ionic⁵ it should also have these atomiclike excitations. Figure 3 shows that the exciton for MgAl $_2$ O $_4$ is in the right place as predicted by the atomic model. The high-energy features in MgAl $_2$ O $_4$ are different than in MgO but are in the same energy range. This difference may simply be a result of the different environments of the Mg $^{2+}$ ion, tetrahedral in MgAl $_2$ O $_4$ and octahedral in MgO, which results in different crystal-field effects. We have developed this model for the Al $L_{2,3}$ SXA also and have found qualitatively similar results. Both the high-energy features and the peak at threshold can be described in terms of atomiclike excitations for each of the oxides studied. For the Al $L_{2,3}$ SXA of α -Al $_2$ O $_3$ each atomic feature had to be shifted 2 eV to higher energy for best comparison.

This atomic excitation model is identical to the models used to describe the $L_{2,3}$ absorption spectra of many transition-metal compounds.^{11,12} For these compounds the SXA spectra are well explained by considering $2p \rightarrow 3d$ atomiclike transitions and crystal-field splitting. The difference between the Mg $^{2+}$ and (Al $^{3+}$) ion electronic structure is the unoccupied s and p levels below the d levels in the Mg $^{2+}$ (Al $^{3+}$) ion. It is not unreasonable to assume that these 3s and 3p levels mix with the O levels to form a conduction band in these oxides. If these conduction-band states were symmetry projected back onto the Mg (Al) core state they would have symmetries of all possible type (s, p, d, \dots) and would appear in the $L_{2,3}$ SXA. We

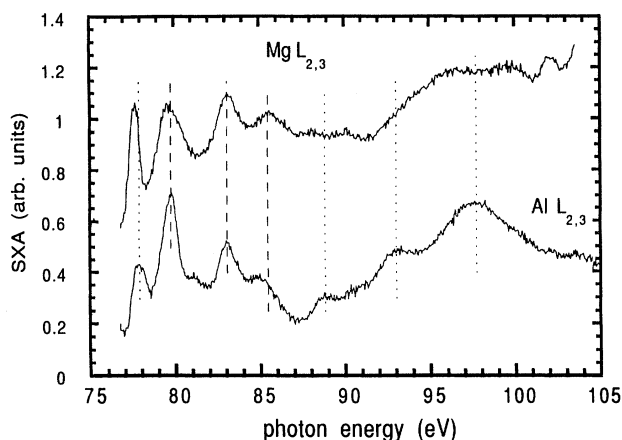


FIG. 7. Comparison of Mg $L_{2,3}$ (top) and Al $L_{2,3}$ (bottom) SXA of MgAl_2O_4 . The Mg $L_{2,3}$ spectrum has been shifted 22.5 eV to achieve the best match of features between threshold and 7 eV above threshold. Dashed lines indicate bandlike features.

therefore suggest that the structure located between the exciton and d states in the SXA spectra of these oxides is due to absorption into conduction-band states. These states are probably affected by the core hole potential and may not give a true representation of the ground-state properties.

Comparing the Mg $L_{2,3}$ and the Al $L_{2,3}$ SXA spectrum of MgAl_2O_4 (Fig. 7) supports this identification. In Fig. 7 the energy scale of the Mg $L_{2,3}$ spectrum is shifted to achieve the best alignment of features between threshold and 7 eV above threshold. Excellent alignment of these features, which are not described by the atomic model, is possible (dashed vertical lines). This is the expected result for band states since they have the same energy throughout the solid. On the other hand, the atomiclike features (exciton and high-energy structure shown by dot-

ted lines in Fig. 7) are localized excitations and are not expected to coincide with features in the other spectrum. Further evidence of the bandlike nature of these features comes from the temperature dependence of the MgO SXA.⁸ Here the phonon coupling was found to be much larger for absorption into the 57.2-eV state than for absorption into the exciton state. This is what would be expected⁸ when comparing the phonon coupling of an excitation involving a core electron into a localized and delocalized state. Based on this analysis, the SXA of these oxides can be broken into three parts, the peak at threshold, the structure up to ≈ 7 eV above threshold, and the structure more than 10 eV above threshold. The structure between threshold and 7 eV above threshold is best described in terms of band structure, while the high-energy structure and the structure at threshold are best described in terms of atomiclike excitations.

SUMMARY AND CONCLUSION

We have investigated the Al $L_{2,3}$ SXE of $\alpha\text{-Al}_2\text{O}_3$ anodized Al_2O_3 and MgAl_2O_4 , the Al $L_{2,3}$ SXA of $\alpha\text{-Al}_2\text{O}_3$ and MgAl_2O_4 , the Mg $L_{2,3}$ SXE of MgO, and the Mg $L_{2,3}$ SXA of MgO and MgAl_2O_4 . We have found that both these techniques would be useful as structural probes for these simple oxides. Comparison of the SXE of MgO and $\alpha\text{-Al}_2\text{O}_3$ to LDA calculations suggests that the final-state rule is obeyed for the SXE of these oxides. The SXA spectra of these oxides can be separated into features due to atomiclike excitations and features due to band structure.

ACKNOWLEDGMENTS

This work was supported by NSF Grant No. DMR-8715430 and the National Institute of Standards and Technology.

*Present address: Synchrotron Radiation Center, Stoughton, WI 53589.

†Present address: Tulane University, New Orleans, LA 70118.

¹U. V. Barth and F. Grossman, *Phys. Rev. B* **25**, 5150 (1982).

²P. Livins and S. E. Schnatterly, *Phys. Rev. B* **37**, 6731 (1988).

³J.-E. Rubensson, D. R. Mueller, R. Shuker, D. L. Ederer, C. H. Zhang, J. Jia, and T. A. Callcott, *Phys. Rev. Lett.* **64**, 1047 (1990).

⁴W. L. O'Brien, J. Jia, Q.-Y. Dong, T. A. Callcott, K. E. Miyano, D. L. Ederer, D. R. Mueller, and C.-C. Kao, *Phys. Rev. Lett.* **70**, 238 (1993).

⁵Y.-N. Xu and W. Y. Ching, *Phys. Rev. B* **43**, 4461 (1991). The symmetry-projected DOS's are from a personal communication with W. Y. Ching.

⁶T. A. Callcott, K. L. Tsang, C. H. Zhang, D. L. Ederer, and E.

T. Arakawa, *Rev. Sci. Instrum.* **57**, 2680 (1989).

⁷W. L. O'Brien, J. Jia, Q.-Y. Dong, T. A. Callcott, J.-E. Rubensson, D. R. Mueller, and D. L. Ederer, *Phys. Rev. B* **44**, 1013 (1991).

⁸W. L. O'Brien, J. Jia, Q.-Y. Dong, T. A. Callcott, D. R. Mueller, and D. L. Ederer, *Phys. Rev. B* **45**, 3882 (1992).

⁹C. E. Moore, *Atomic Energy Levels*, Natl. Bur. Stand. (U.S.) No. 467 (U.S. GPO, Washington, DC, 1949).

¹⁰P. F. Gruzdev and A. V. Loginov, *Opt. Spektrosk.* **45**, 1050 (1978) [*Opt. Spectrosc. (USSR)* **45**, 846 (1978)].

¹¹F. M. F. de Groot, J. C. Fuggle, B. T. Thole, and G. A. Sawatzky, *Phys. Rev. B* **42**, 5459 (1990).

¹²F. M. F. de Groot, J. C. Fuggle, B. T. Thole, and G. A. Sawatzky, *Phys. Rev. B* **41**, 928 (1990).